First-in-Human Phase I study of CTT1057, a Novel [18]F Labeled Imaging Agent with Phosphoramidate Core Targeting Prostate Specific Membrane Antigen in Prostate Cancer

Spencer C. Behr *[#1], Rahul Aggarwal[#2], Henry F. VanBrocklin [1], Robert R. Flavell[1], Kenneth Gao[1], Eric J Small[2, 3], Joseph Blecha[1], Salma Jivan[1], Thomas A. Hope[1], Jeffry P. Simko[4], John Kurhanewicz[1], Susan M. Noworolski[1], Natalie J. Korn[1], Romelyn De Los Santos[4], Matthew R. Cooperberg[3], Peter R. Carroll[3], Hao G. Nguyen[3], Kirsten L. Greene[3], Beatrice Langton-Webster[5], Clifford E. Berkman[5], and Youngho Seo[1].

\# Co-Primary Authors, each contributed equally to this work.

Short Running Title: CTT1057 in prostate cancer

1 – Department of Radiology and Biomedical Imaging, University of California, San Francisco, San Francisco, CA.

2 – Department of Medicine, University of California, San Francisco, San Francisco, CA.

3 – Department of Urology, University of California, San Francisco, San Francisco, CA.

4 – Department of Pathology, University of California, San Francisco, San Francisco, CA.

5 – Cancer Targeted Technology, Woodinville, WA

* - Corresponding Author:

Spencer C. Behr, M.D.

Associate Professor of Radiology

Department of Radiology and Biomedical Imaging

University of California, San Francisco

505 Parnassus Ave, Box 0628

San Francisco, CA 94143

Phone #: 415-353-1821

Fax #:415-476-4791

Email: spencer.behr@ucsf.edu

Word count of manuscript: 4,996

ABSTRACT

Prostate-specific membrane antigen (PSMA) targeting agents comprise a rapidly emerging class of radiopharmaceuticals for prostate cancer diagnostic imaging. Unlike most other PSMA agents with a urea-backbone, CTT1057 is based on a phosphoramidate scaffold that irreversibly binds to PSMA. We conducted a first-in-human Phase I study of CTT1057 in patients with localized and metastatic prostate cancer.

Methods: Two patient cohorts were recruited. Cohort A patients had biopsy-proven localized prostate cancer preceding radical prostatectomy, and cohort B were patients with metastatic castrate resistant prostate cancer. Cohort A patients were imaged on multiple time points after intravenous injection with 362 ± 8 MBq CTT1057 to evaluate the kinetics of CTT1057 and estimate radiation dose profiles. Mean organ-absorbed doses and effective doses were calculated. CTT1057 uptake in the prostate gland and regional lymph nodes was correlated with pathology, PSMA staining, and results of conventional imaging. In cohort B, patients were imaged 60 to 120 minutes after injection of CTT1057. PET images were assessed for overall image quality, and areas of abnormal uptake contrasted with conventional imaging.

Results: In cohort A (n=5), the average total effective dose was 0.023 mSv/MBq. The kidneys exhibited the highest absorbed dose, 0.067 mGy/MBq. The absorbed dose of the salivary glands was 0.015 mGy/MBq. For cohort B (n=15), CTT1057-PET detected 97 metastatic lesions, and 44 of 56 bone metastases detected on CTT1057-PET (78.5%) were also detectable on bone scan. Eight of 32 positive lymph nodes visualized on CTT1057-PET (25%) were enlarged by size criteria on CT.

Conclusion: CTT1057 is a promising novel phosphoramidate PSMA-targeting ^{18}F-labeled PET radiopharmaceutical that demonstrates similar biodistribution to urea-based PSMA-targeted agents with lower exposure to the kidneys and salivary glands. CTT1057 detects metastatic lesions with higher sensitivity than conventional imaging. Further prospective studies with CTT1057 are warranted to elucidate its role in cancer imaging.

INTRODUCTION

Early and accurate diagnosis of prostate cancer is essential for proper patient management. Contrast-enhanced computer tomography (CT) and radionuclide bone scan are employed for staging and restaging. However, more sensitive and accurate imaging tests are needed as compared to current standard of care exams (1-4).

Positron emission tomography (PET) imaging is an enticing choice as it offers the potential to both stage patients and provide insight into tumor biology. Prostate-specific membrane antigen (PSMA) is a very promising target as it is overexpressed in both primary tumor and metastatic lesions. Recently, urea-based PSMA-targeting agents such as ^{68}Ga-PSMA-11 have shown promise in prostate cancer imaging (5-7).

Fluorine-18 labeled agents such as ^{18}F-DCFPyL (8) and ^{18}F-PSMA-1007 (9) have also entered clinical development. F-18 offers several advantages over Ga-68. First, cyclotron production of F-18 enables large-scale batches. Second, F-18 has a longer half-life than Ga-68 (110 minutes vs. 68 minutes), simplifying transport and may allow for more delayed imaging. Third, the shorter positron range of F-18 compared to that of Ga-68 provides improved image quality.

CTT1057 is a peptidomimetic incorporating a phosphoramidate scaffold (Fig. 1), resulting in irreversible binding to PSMA and improved tumor uptake shown in preclinical models (10). Hence, the different biodistribution of CTT1057 from that of other urea-based agents is worth careful investigation, particularly for developing a corresponding PSMA-targeted therapeutic radiopharmaceutical. Salivary glands and kidneys are organs at risk when a urea-based PSMA-targeting radiopharmaceutical

therapy is applied; thus dose profiles in these organs are of great importance for developing a new PSMA imaging agent like CTT1057.

In this first-in-human Phase I study, the safety, biodistribution, radiation dosimetry and histopathologic correlation were evaluated in men prior to prostatectomy, and the utility of CTT1057 in detecting PSMA-avid metastases was assessed in patients with metastatic castrate-resistant prostate cancer (mCRPC). Furthermore, a comparison of different absorbed doses in organs between CTT1057 and several other PSMA imaging agents was made.

MATERIALS AND METHODS

This prospective study was performed after approval of the local Institutional Review Board, and approval of the Food and Drug Administration under an investigational new drug application held by Cancer Targeted Technology (IND 124021) and registered as NCT02916537.

Preparation of CTT1057

CTT1057 was prepared under current good manufacturing practice at our institution. CTT1057 production was carried out on an ORA Neptis® Perform synthesizer (Optimized Radiochemical Applications, Philippeville, Belgium) coupling succinimidyl-^{18}F-fluorobenzoate to the primary amine precursor CTT1298, as previously described (11).

Patient Characteristics and Study Design

Written informed consent was obtained from each patient prior to radiotracer administration. Key inclusion criteria included Eastern Cooperative Oncology Group performance status of 0 or 1, histologically confirmed adenocarcinoma of the prostate and adequate hematologic and organ function. In cohort A, patients had to be deemed eligible for radical prostatectomy within 12 weeks following CTT1057-PET. No systemic anti-cancer therapy was allowed prior to imaging including androgen

deprivation, chemotherapy, or investigational systemic therapy. In cohort B, patients were required to have mCRPC defined by prostate cancer working group 2 criteria with at least three metastatic lesions seen on CT or MRI of the chest/abdomen/pelvis and/or radionuclide bone scan performed within 12 weeks of CTT1057-PET. Key exclusion criteria for both cohorts included any other radionuclide within 5 physical half-lives, histologic evidence of small cell/neuroendocrine prostate cancer in > 50% of biopsy tissue, or history of invasive secondary malignancies within 12 months. Safety assessments included serial monitoring of vital signs, injection site, adverse event assessment on the day of scan up to 6 hours, and telephone at 7 days following CTT1057-PET.

Imaging Protocol for Cohort A

All PET scans were performed on a 3-tesla time-of-flight (TOF) PET/MR system (SIGNA PET/MR, GE Healthcare, Waukesha, WI). Three-dimensional PET data were acquired in list-mode with varying time per bed as time progressed for 6 bed positions. PET images were reconstructed with matrix size 192×192, 28 subsets and 3 iterations of TOF ordered-subsets expectation maximization algorithm, 5 mm full-width at half-maximum in-plane Gaussian postreconstruction filter, and point-spread-function model. Attenuation correction for PET reconstruction was performed using the MR-based attenuation correction (MRAC) technique provided by the scanner manufacturer. Full body MR images were axial MRAC images, two-point Dixon 3D fast spoiled gradient recalled echo, axial variable flip-angle single shot fast spin echo T2-weighted images,

and axial diffusion weighted images. Patients without a clinical prostate MR exam within 12 weeks of this study, received a mpMR exam with an endorectal coil (12). Dedicated pelvic MR sequences included axial 3D, reduced field of view T2 weighted imaging multiple diffusion-weighted imaging (b=0, 600 and 1400), and axial T1-weighted imaging.

The administered mass of CTT1057 was 4.01 ± 3.20 μg (range $1.49 - 8.83$). The administered activity was 362 ± 8 MBq (range $352 - 370$ MBq).

Six PET bed positions were acquired to cover vertex to mid thighs. A total of 6 sequential PETs were acquired for each patient (i.e., PET1 through PET6). Acquisition durations were 1 minute/bed for PET1&2, 2 minutes/bed for PET3&4, 4 minutes/bed for PET5&6. PET1 through PET4 were acquired immediately after administration of CTT1057 without any interruptions. PET5 was started approximately 50 to 80 minutes postinjection. PET6 was acquired approximately 100 minutes after PET5. Between PET5 and PET6, dedicated MR pelvic images were acquired as described earlier. Patients were encouraged to void during breaks, but this was not mandated.

Imaging Protocol for Cohort B

For cohort B, only one static scan 60 to 120 minutes after administration of 369.83 ± 7 MBq of CTT1057 (range $355.2 - 381.1$ MBq) was acquired with a 3 minute/bed for 6 bed positions. The PET reconstruction parameters for cohort B were same as for cohort A. The full body MR examination was performed without intravenous contrast with the same protocol for cohort A.

Radiation Dosimetry for Cohort A

From PET1 through PET6, time-activity data were generated for brain, lungs, heart, liver, gallbladder, spleen, kidneys, and urinary bladder. Using the average male organ mass and density values, the mean activity concentrations multiplied by the volumes of each organ were used as the total activities. Residence times were derived by curve-fitting the time-activity data. The data fitting and dose calculations were performed on OLINDA|EXM (version 1.1, Vanderbilt University). The absorbed dose to each organ (mGy/MBq), and the ICRP 60 effective dose (mSv/MBq) were tabulated. Finally, organ-specific absorbed dose was estimated using a sphere model implemented in OLINDA 1.1 for salivary and lacrimal glands.

Radiology-Pathology Primary Tumor Assessment for Cohort A

Under the guidance of a pathologist (JPS), the resected prostates were weighed, measured, inked, infiltrated with 400 cc of 10% buffered formalin using a syringe, and then fixed overnight in a 10% neutral buffered formalin bath. The prostates were sliced at 3-mm intervals perpendicular to the urethra using a customized slicer that was designed for this purpose, the apical sides of all sections were placed down in their respective tissue cassettes (to preserve orientation) and processed and cut as whole-mount sections. Slides were evaluated using a conventional light microscope with all tumors marked and

characterized as to tumor Gleason score, percent of various Gleason grades and tumor growth patterns.   The slides were subsequently digitized on a high-resolution flatbed scanner for digital overlapping with the radiographic images. For immunohistochemical assessment, tissues were sectioned at 4 micrometer, heat-induced epitope retrieval with a citrate buffer and using streptavidin horseradish perooxidase were used. PSMA expression in the primary prostate tumors was assessed using a mouse monoclonal antibody to PSMA (clone 3E6, Dako).

Whole Body Image Analysis

Two board-certified nuclear medicine physicians (RRF and SCB) with 7 and 12 years of PET experience, respectively, reviewed all PET images on an Advantage Workstation (GE Healthcare, Waukesha, Wisconsin). MRAC, non-AC-corrected images, and MR images were reviewed.

For cohort A, each PET time point was assessed for focal radiotracer uptake in the prostate. Uptake was considered positive if uptake was clearly above adjacent prostatic parenchyma. For each focal CTT1057-avid lesion, a region of interest (ROI) was drawn to encompass the lesion with care to exclude the urinary bladder. This ROI was then propagated to the other PET time points and the SUV_{max} was recorded. If no focal uptake was clearly seen above background, an ROI was drawn in the location of the tumor based on pathology and mpMRI. Blood pool and muscle uptake were calculated by drawing a 1 cm ROI and recording the SUV_{mean} in the ascending aorta for blood pool and right gluteal musculature for muscle. The ratio of tumor to blood pool and tumor to musculature was

calculated at each PET time point. PSMA-avid lymph nodes were considered positive if PSMA uptake was clearly above adjacent blood pool and in the expected location of a lymph node on cross sectional imaging.

For cohort B, SUV_{mean}'s calculated for multiple normal organs for each patient by drawing a 1 cm ROI. The anatomic locations and SUV_{max}'s were determined for each identifiable metastatic lesion, with up to five lesions per organ. Lesion to background ratios (i.e., tumor SUV_{max} to SUVmean for liver, blood pool, and muscle) were calculated. Additionally, each NM physician qualitatively scored each study using a Visual Analog Scale (VAS) of 1 to 100 (1 = non-diagnostic, 100= perfect study).

RESULTS

Patient Characteristics and Safety Results

A total of 20 patients were enrolled (cohort A: n=5; cohort B: n=15). Supplemental Table 1 summarizes individual patient characteristics, surgical pathology, and CTT1057 imaging results for cohort A. Supplemental Table 2 summarized patient characteristics, prior treatment and PSA levels for cohort B. Average ages were similar between cohorts. In cohort A, patients had Gleason 3+4 (n=3) or Gleason 4+3 (n=2) patterns, the mean PSA 12.29 ng/mL (range 4 – 38.76). In cohort B, the mean PSA was 49.2 ng/mL (range 0.7 – 1238.6), and all were receiving ongoing androgen deprivation therapy. Nine patients (60%) had received prior treatment with abiraterone and/or enzalutamide. All 15 patients had definitive local therapy – five (33%) prior radical

prostatectomy and 10 (67%) had undergone prostate radiation without or with pelvic radiation.

No adverse events or changes in vitals were associated with CTT1057 injection in the study.

Biodistribution for Cohort A

PET images demonstrated uptake within the salivary glands, lacrimal glands, liver, spleen and proximal small bowel (Fig. 2). Blood pool activity progressively decreased at 90 to 120 minutes postinjection with rapid excretion through kidneys into urinary bladder. In 4 of the 5 patients, biliary excretion was noted.

Radiation Dosimetry for Cohort A

The effective dose was estimated at 0.023±0.007 mSv/MBq (Table 1). A factor for the variation of estimated effective doses between patients was the absorbed dose in urinary bladder. Table 2 also shows the dose comparison to three other PSMA-targeted PET imaging agents, ^{68}Ga-PSMA-11(13), ^{18}F-DCFPyL (8), and ^{18}F-PSMA-1007 (9). The estimated absorbed doses in salivary and lacrimal glands were 0.0146 and 0.00732 mGy/MBq, respectively.

Primary Tumor Analysis for Cohort A

Four patients had CTT1057-avid prostate lesions corresponding to the pathology-proven cancer. The one patient without focal prostatic PSMA uptake had a PSA of 4 ng/dL and Gleason 3+4. The highest uptake in the primary tumors was seen at PET5 and PET6 (Fig. 3).

A total of 68 lymph nodes were resected during surgery from the five patients. None of these lymph nodes was macroscopically positive; one node had microscopic metastatic disease (less than 0.2 mm). This patient had the highest PSA (38.76 ng/mL) and Gleason 4+3.

Qualitative and Quantitative Image Analysis for Cohort B

The average VAS score of CTT1057 images was 76 ± 5.4. The normal organ uptake of CTT1057 is shown in Supplemental Table 3.

All 15 patients had evidence of at least one PSMA-avid metastasis on CTT1057-PET. In total, 97 PSMA-avid lesions were evaluated, with an average of 6.5 lesions/patient. The median SUV_{max} of the lesions was 12.17 (IQR 5.9 – 19.02). The distribution of metastatic sites detected by CTT1057-PET is shown in Table 3. CTT1057 demonstrated improved sensitivity for bone and lymph node detection compared to conventional bone scan and CT of the chest/abdomen/pelvis. This result is consistent with other reports that showed improved detection rates of bone metastases over bone scan by PSMA-PET (14). Of the 56 positive bone metastases detectable on CTT1057, 44

14

(78.5%) were detectable on bone scan. Of the 32 positive lymph nodes on CTT1057, only

eight (25%) were enlarged by size criteria on baseline CT imaging. All CT enlarged

lymph nodes (>1.5 cm in short axis) were positive on CTT1057. Three lesions were seen

on bone scan only without corresponding CTT1057 uptake. See Figure 4 for examples of

CTT1057-avid osseous and lymph node metastases. Two patients who received

CTT1057-PET subsequently underwent metastatic tumor biopsy of a PSMA-avid lesion

for purposes of clinical care. In both cases, the CT-guided core needle biopsy was

positive for prostate cancer and contained sufficient tumor material to permit

histopathologic evaluation (Supplemental Fig. 1).

DISCUSSION

This first-in-human study demonstrates that this novel, phosphoramidate-based PSMA targeted imaging agent, CTT1057 is safe with no adverse reactions. Furthermore, CTT1057 both accurately identify the primary prostate cancer observed on pathologic examination of radical prostatectomy specimens as well as detect osseous and lymph node metastases with improved sensitivity compared to conventional imaging.

The biodistribution of CTT1057 showed similar characteristics to that of other PSMA PET agents. Overall, there is high salivary, renal and urinary bladder uptake. The high renal uptake is likely a combination of the PSMA expression as well excretion of radiotracer, which resulted in high accumulation of radiotracer in the urinary bladder, which is similar to that of reported for both ^{68}Ga-based and ^{18}F-based PSMA agents (8,15). Unlike the other urea-based PSMA agents, we observed only minimal radiotracer in the small bowel. Additionally, a high number of patients imaged with CTT1057 had biliary excretion of the radiotracer, which was rarely reported with the urea-based radiotracers until the recently with PSMA-1007 (9). Our data indicate that delayed imaging 90 minutes or later would be preferred, which is in line with other PSMA-PET agents. However, unlike PSMA-1007 (9), CTT1057 is similar to other PSMA-based agents in the high accumulation within the urinary bladder, which is a potential limitation as it could obscure adjacent lesions in the prostate or regional pelvic lymph nodes.

As detailed in Table 4, the effective dose from CTT1057 of 0.0231 mGy/MBq was similar to those reported for ^{68}Ga-PSMA-11 (15) and ^{18}F-PSMA-1007(9) and moderately higher than ^{18}F-DFCPyL (8). When compared to radiation sensitive organs

like red marrow and breast tissue, the absorbed dose was less than ^{68}Ga-PSMA-11 and ^{18}F-PSMA-1007 and similar to ^{18}F-DFCPyL. The effective dose of CTT1057 was increased by the significant urinary accumulation. For example, when the urinary bladder dose was simulated to have the same dose from ^{18}F-DCFPyL, the effective dose scaled down to 0.014 mSv/MBq. Future studies with oral hydration, intravenous furosemide, and voiding prior to imaging could decrease the overall effective dose, and absorbed doses to the testes and urinary bladder.

In comparison to the data reported only for salivary glands, the dose (0.0146 mGy/MBq) from CTT1057 is significantly lower than the dose (0.0610 mGy/MBq) from ^{68}Ga-PSMA I&T (16). Xerostomia has also been shown to be the dose-limiting toxicity in clinical trials with urea-based PSMA-617 (17,18). Since the same phosphoramidate binding scaffold is being pursued as a therapeutic PSMA-targeted agent, this is an important finding that could potentially reduce complications to salivary and lacrimal glands during radionuclide therapy. Additionally, the absorbed dose of CTT1057 in the kidneys was less than reported with for the other three PSMA based agents (8,9,19).

All five enrolled preprostatectomy patients had Gleason patterns of 7. In four, PSMA uptake was clearly seen above background in the primary tumors (Supplemental Fig. **2**) and PSA levels were less than 10 ng/mL The most intense uptake in the primary tumor by CTT1057 also had the highest PSA levels (38.8) and a Gleason pattern of 4+3 (Supplemental Fig. **3**). These findings are consistent with those recently reported by Uprimny et al. (20). The overall assessment for the sensitivity for lymph node detection was limited as this study was primary performed for dosimetry and safety. Of the 68 lymph nodes resected, there was no macroscopic disease, and only one node had

microscopic metastases (less than 0.2 mm of disease). This lymph node did not demonstrate any significant uptake of CTT1057, which may be due to minimal amount of disease present, and below the threshold for PET imaging (21-23).

In the mCRPC cohort, more lesions were detected with CTT1057-PET-based imaging than compared to conventional CT or bone scan. Despite the limitation of pathologic confirmation of PSMA-avid lesions, the results support future studies with CTT1057 for routine clinical care in this setting. In patients with oligometastatic CRPC, when consideration is frequently made for the focal targeting of metastases with radiation, improved sensitivity of lesion detection permits more comprehensive and accurate targeting of detectable metastases. In addition, the choice of systemic therapy can differ in nonmetastatic versus mCRPC, and earlier detection of metastases enables the earlier institution of recommended therapies for mCRPC, including abiraterone, enzalutamide, and other agents in clinical development. Conversely, the absence of PSMA uptake in osseous lesions detectable on conventional bone scan may signify a metabolically inactive tumor indicative of therapeutic response. These hypotheses warrant evaluation in future prospective studies in the mCRPC setting.

The degree of intratumoral uptake of CTT1057 appears to be comparable to other PSMA-targeted tracers in clinical development, including ^{68}Ga-PSMA-11(24-26).The high uptake of CTT1057 in both osseous and soft tissue metastases, at significantly higher levels than that observed in normal organs and blood pool, provide a strong justification for the development of a therapeutic PSMA-targeted radiopharmaceutical based on a similar chemical scaffold as a theranostic pair. ^{177}Lu-labeled CTT1403, based

on the same PSMA-binding scaffold as CTT1057, is currently in preclinical testing (27) and is slated to begin clinical trials shortly.

CONCLUSION

Overall, CTT1057 is a promising novel PSMA-targeting ^{18}F-labeled PET imaging agent based on a phosphoramidate core that is safe without any radiotracer-related adverse reactions. The biodistribution of CTT1057 is similar to those of other PSMA-targeted agent, and exposure rates of CTT1057 are also similar to those of the urea-based PET compounds with the exception of lower exposure to kidneys and salivary glands, which may be significant for future therapeutic considerations. Future larger cohort studies are needed to determine CTT1057's sensitivity and specificity for detection of metastases.

REFERENCES

1. Blomqvist L, Carlsson S, Gjertsson P, et al. Limited evidence for the use of imaging to detect prostate cancer: a systematic review. *Eur J Radiol.* 2014;83:1601-1606.

2. Hricak H, Dooms GC, Jeffrey RB, et al. Prostatic carcinoma: staging by clinical assessment, CT, and MR imaging. *Radiology.* 1987;162:331-336.

3. Scheidler J, Hricak H, Vigneron DB, et al. Prostate cancer: localization with three-dimensional proton MR spectroscopic imaging--clinicopathologic study. *Radiology.* 1999;213:473-480.

4. Shinohara K, Wheeler TM, Scardino PT. The appearance of prostate cancer on transrectal ultrasonography: correlation of imaging and pathological examinations. *J Urol.* 1989;142:76-82.

5. Udovicich C, Perera M, Hofman MS, et al. (68)Ga-prostate-specific membrane antigen-positron emission tomography/computed tomography in advanced prostate cancer: Current state and future trends. *Prostate Int.* 2017;5:125-129.

6. Schmidt-Hegemann NS, Fendler WP, Buchner A, et al. Detection level and pattern of positive lesions using PSMA PET/CT for staging prior to radiation therapy. *Radiat Oncol.* 2017;12:176.

7. Chang SS. Overview of prostate-specific membrane antigen. *Rev Urol.* 2004;6 Suppl 10:S13-18.

8. Szabo Z, Mena E, Rowe SP, et al. Initial Evaluation of [(18)F]DCFPyL for Prostate-Specific Membrane Antigen (PSMA)-Targeted PET Imaging of Prostate Cancer. *Mol Imaging Biol.* 2015;17:565-574.

9. Giesel FL, Hadaschik B, Cardinale J, et al. F-18 labelled PSMA-1007: biodistribution, radiation dosimetry and histopathological validation of tumor lesions in prostate cancer patients. *Eur J Nucl Med Mol Imaging.* 2017;44:678-688.

10. Ganguly T, Dannoon S, Hopkins MR, et al. A high-affinity [(18)F]-labeled phosphoramidate peptidomimetic PSMA-targeted inhibitor for PET imaging of prostate cancer. *Nucl Med Biol.* 2015;42:780-787.

11. Jivan S, Neuman K, Villeret G, et al. Fully automated preparation of [18F]CTT1057, a new prostate cancer imaging agent, prepared using the ORA Neptis® Perform Synthesizer. . *J Labelled Comp Radiopharm* 2017;60:1.

12. Starobinets O, Korn N, Iqbal S, et al. Practical aspects of prostate MRI: hardware and software considerations, protocols, and patient preparation. *Abdom Radiol (NY).* 2016;41:817-830.

13. Eder M, Neels O, Muller M, et al. Novel Preclinical and Radiopharmaceutical Aspects of [68Ga]Ga-PSMA-HBED-CC: A New PET Tracer for Imaging of Prostate Cancer. *Pharmaceuticals (Basel).* 2014;7:779-796.

14. Zacho HD, Nielsen JB, Haberkorn U, Stenholt L, Petersen LJ. (68) Ga-PSMA PET/CT for the detection of bone metastases in prostate cancer: a systematic review of the published literature. *Clin Physiol Funct Imaging.* 2017.

15. Afshar-Oromieh A, Zechmann CM, Malcher A, et al. Comparison of PET imaging with a (68)Ga-labelled PSMA ligand and (18)F-choline-based PET/CT for the diagnosis of recurrent prostate cancer. *Eur J Nucl Med Mol Imaging.* 2014;41:11-20.

16. Herrmann K, Bluemel C, Weineisen M, et al. Biodistribution and radiation dosimetry for a probe targeting prostate-specific membrane antigen for imaging and therapy. *J Nucl Med.* 2015;56:855-861.

17. Kratochwil C, Bruchertseifer F, Rathke H, et al. Targeted alpha-Therapy of Metastatic Castration-Resistant Prostate Cancer with (225)Ac-PSMA-617: Dosimetry Estimate and Empiric Dose Finding. *J Nucl Med.* 2017;58:1624-1631.

18. Hofman MS, Violet J, Hicks RJ, et al. [(177)Lu]-PSMA-617 radionuclide treatment in patients with metastatic castration-resistant prostate cancer (LuPSMA trial): a single-centre, single-arm, phase 2 study. *Lancet Oncol.* 2018;19:825-833.

19. Afshar-Oromieh A, Hetzheim H, Kubler W, et al. Radiation dosimetry of (68)Ga-PSMA-11 (HBED-CC) and preliminary evaluation of optimal imaging timing. *Eur J Nucl Med Mol Imaging.* 2016;43:1611-1620.

20. Uprimny C, Kroiss AS, Decristoforo C, et al. (68)Ga-PSMA-11 PET/CT in primary staging of prostate cancer: PSA and Gleason score predict the intensity of tracer accumulation in the primary tumour. *Eur J Nucl Med Mol Imaging.* 2017;44:941-949.

21. Park SY, Zacharias C, Harrison C, et al. Gallium 68 PSMA-11 PET/MR Imaging in Patients with Intermediate- or High-Risk Prostate Cancer. *Radiology.* 2018;288:495-505.

22. Mottaghy FM, Heinzel A, Verburg FA. Molecular imaging using PSMA PET/CT versus multiparametric MRI for initial staging of prostate cancer: comparing apples with oranges? *Eur J Nucl Med Mol Imaging.* 2016;43:1397-1399.

23.   Grubmuller B, Baltzer PA, Hartenbach S, et al. PSMA ligand PET/MRI for primary prostate cancer: Staging performance and clinical impact. *Clin Cancer Res.* 2018.

24.   Afshar-Oromieh A, Malcher A, Eder M, et al. PET imaging with a [68Ga]gallium-labelled PSMA ligand for the diagnosis of prostate cancer: biodistribution in humans and first evaluation of tumour lesions. *Eur J Nucl Med Mol Imaging.* 2013;40:486-495.

25.   Cho SY, Gage KL, Mease RC, et al. Biodistribution, tumor detection, and radiation dosimetry of 18F-DCFBC, a low-molecular-weight inhibitor of prostate-specific membrane antigen, in patients with metastatic prostate cancer. *J Nucl Med.* 2012;53:1883-1891.

26.   Morigi JJ, Stricker PD, van Leeuwen PJ, et al. Prospective Comparison of 18F-Fluoromethylcholine Versus 68Ga-PSMA PET/CT in Prostate Cancer Patients Who Have Rising PSA After Curative Treatment and Are Being Considered for Targeted Therapy. *J Nucl Med.* 2015;56:1185-1190.

27.   Choy CJ, Ling X, Geruntho JJ, et al. (177)Lu-Labeled Phosphoramidate-Based PSMA Inhibitors: The Effect of an Albumin Binder on Biodistribution and Therapeutic Efficacy in Prostate Tumor-Bearing Mice. *Theranostics.* 2017;7:1928-1939.
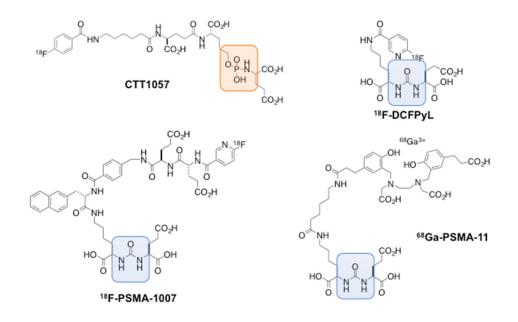
FIGURES

Figure 1. Chemical structure of CTT1057 with comparison to other urea-based PSMA PET agents - [18]F –DCFPyL, ^{18}F-PSMA-1007 and ^{68}Ga-PSMA-11. Orange highlighted area outlines the phosphoramidate backbone in CTT1057 and blue area highlights the urea backbone in the other three agents.
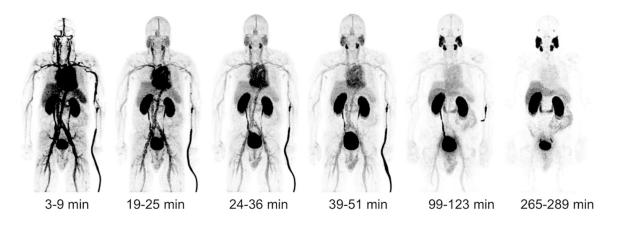
Figure 2. Maximum Intensity Projection (MIP) PET images from patient #003. This patient was a 73-year old male pre-prostatectomy patient who had Gleason 3+4 prostate cancer and PSA of 6.7 ng/ml 2 weeks prior to imaging. Patient did not have any PSMA-avid lymph node or metastases at time of imaging. Surgery performed 12 weeks after imaging confirmed disease localized to the prostate with no lymph node involvement. Note the activity adjacent to the left arm due to radiotracer.
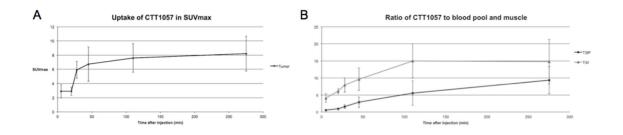
Figure 3. CTT1057 uptake in the primary prostate tumors over time. (A)

Comparison of average SUVmax over multiple PET times points for all tumors. (B)

Graph of ratio of tumor to blood pool (T:BP), and tumor to muscle (T:M) over time of the

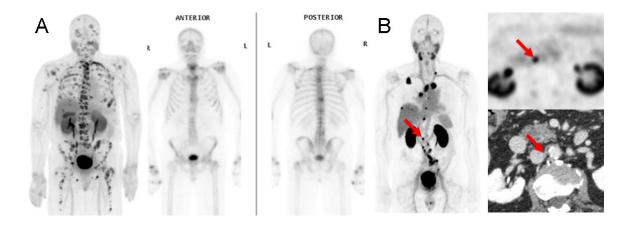six CTT1057 avid tumors. Error bars indicate standard deviation.

Figure 4. Example of CTT1057 avid osseous and lymph lesions from the Cohort B group. (A) CTT1057 MIP PET (left) and anterior (middle) and posterior (right)Tc99m-HDP planar bone scan. Example of a patient with extensive CTT1057 avid osseous metastatic disease and only minimal uptake on the standard of care bone scan. (B) CTT1057 MIP PET (left), axial PET (top right) and axial CT (bottom right) highlights a patient with four millimeter short lymph node that is not enlarged by size criteria on conventional CT, but displays marked CTT1057 uptake indicative of a high likelihood of metastatic involvement.

Table 1. Radiation dose estimates (OLINDA 1.1, ICRP60) of CTT1057

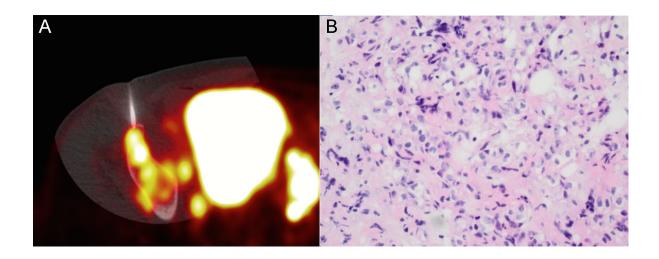| Absorbed Dose (mGy/MBq)			
Adrenals	0.009	±	0.001
Brain	0.006	±	0.000
Breasts	0.005	±	0.001
Gallbladder Wall	0.014	±	0.001
LLI Wall	0.013	±	0.003
Small Intestine	0.010	±	0.001
Stomach Wall	0.007	±	0.001
ULI Wall	0.009	±	0.001
Heart Wall	0.018	±	0.001
Kidneys	0.067	±	0.001
Liver	0.016	±	0.000
Lungs	0.013	±	0.001
Muscle	0.007	±	0.001
Pancreas	0.009	±	0.001
Red Marrow	0.007	±	0.001
Osteogenic Cells	0.009	±	0.002
Skin	0.005	±	0.001
Spleen	0.016	±	0.001
Testes	0.010	±	0.002
Thymus	0.007	±	0.001
Thyroid	0.005	±	0.001
Urinary Bladder Wall	0.259	±	0.126
Effective Dose (mSv/MBq)	0.023	±	0.007

Table 2. Comparison of organ and absorbed and effective dose estimates for CTT1057 compared to those of ^{68}Ga-PSMA-11(13), ^{18}F-DCFPyL(8) and ^{18}F-PSMA-1007(9).

Absorbed Dose (mGy/MBq)				
Organ	18F-CTT1057	68Ga-PSMA-11	18F-DCFPyL	18F-PSMA-1007
	This work	Afshar-Oromieh et al.	Szabo et al.	Giesel et al.
Adrenals	9.32E-03	1.42E-02	3.11E-02	1.94E-02
Brain	5.79E-03	9.00E-03	2.19E-02	7.20E-03
Breasts	5.06E-03	8.80E-03	4.57E-03	8.06E-03
Gallbladder Wall	1.43E-02	1.44E-02	1.44E-02	2.22E-02
LLI Wall	1.35E-02	1.23E-02	1.05E-02	4.83E-02
Small Intestine	9.72E-03	1.63E-02	9.13E-03	1.56E-02
Stomach Wall	7.47E-03	1.20E-02	1.16E-02	1.42E-02
ULI Wall	9.08E-03	5.40E-02	1.67E-02	4.08E-02
Heart Wall	1.78E-02	1.09E-02	1.29E-02	2.51E-02
Kidneys	6.74E-02	1.62E-01	9.45E-02	1.70E-01
Liver	1.59E-02	3.09E-02	3.80E-02	6.05E-02
Lungs	1.33E-02	1.02E-02	1.08E-02	1.11E-02
Muscle	7.44E-03	1.05E-02	6.32E-03	1.00E-02
Pancreas	9.10E-03	1.38E-02	2.44E-02	1.92E-02
Red Marrow	6.95E-03	9.20E-03	1.04E-02	1.33E-02
Osteogenic Cells	9.10E-03	1.42E-02	9.58E-03	1.55E-02
Skin	4.94E-03	8.85E-02	4.05E-03	7.30E-03
Spleen	1.61E-02	4.46E-02	1.85E-02	7.39E-02
Testes	9.86E-03	1.04E-02	1.01E-02	8.37E-03
Thymus	6.72E-03	9.90E-03	5.56E-03	9.90E-03
Thyroid	5.47E-03	9.70E-03	8.56E-03	8.50E-03
Urinary Bladder Wall	2.59E-01	1.30E-01	8.64E-02	1.87E-02
Effective Dose (mSv/MBq)	**2.28E-02**	**2.36E-02**	**1.39E-02**	**2.20E-02**

Table 3. Metastatic sites of uptake on CTT1057 and conventional imaging

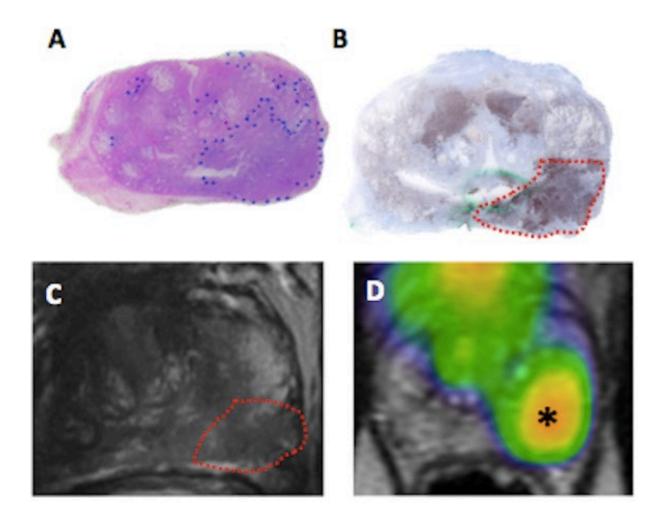|	CTT1057-PET			Whole body bone scan	CT Chest/Abd/Pelvis
	#	Median SUVmax	IQR	#	Size in cm* (range)
Lymph Node	32	11.28	5.98-23.99	N/A	0.9 (0.4 – 2.8)
Bone	56	12.96	7.32 – 18.52	44 (78.5%)	N/A
Prostate Bed	3	14.09	13.64 – 25.8	N/A	1.43 (1.2 – 1.7)
Lung	6	3.16	2.65 – 5.45	N/A	1.2 (0.8 -2.1)

* Measurements were performed in long axis measurements except for lymph nodes which were measured along short axis.

Supplemental Figure 1. Examples biopsied CTT1057 avid confirmed prostate metastases. (A) Fused CTT1057-PET with CT images from the bone biopsy from one of the cohort B patients demonstrating the needle core through the PSMA avid osseous metastasis. (B) H&E pathology section confirming metastatic prostate cancer.

Supplemental Figure 2. (A) Whole-mount H&E pathology slide, (B) immunohistology slide with PSMA-antibody and (C) axial T2-weighted imaging demonstrating bilateral Gleason 3+4 prostate cancers in the bilateral peripheral zone (dashed lines) from patient 001 - a 57-year old man with a PSA of 6 ng/mL. (D) Fused CTT1057-PET on the T2-weighted image with corresponding CTT1057 uptake in these tumors (*).

Supplemental Figure 3. (A) Whole-mount H&E pathology slide, (B) immunohistology slide with PSMA-antibody and (C) axial T2-weighted imaging demonstrating a Gleason 4+3 prostate cancer in the left peripheral zone (dashed line) from patient 004 - a 61-year old man with a PSA of 38.8 ng/mL. (D) Fused CTT1057-PET from PET5 overlaid on the T2-weighted MRI showing focal CTT1057 uptake corresponding to this tumor (*)

Supplemental Table 1. Cohort A - Demographic information, pathology and CTT1057 uptake (SUV_{max}) in the primary prostate cancers.

Pt #	Age	PSA	Final Pathology	Focal PSMA uptake?	PET1	PET 2	PET3	PET 4	PET 5	PET6
001	57	6	Gleason 3+4	yes	5.1	5.9	4.3	*	10.7	9.6
			Gleason 3+4	yes	4.4	4.4	2.7	*	4	6
002	63	6.7	Gleason 4+3	yes	3.9	4.6	5.4	6	9.6	10.2
003	73	4	Gleason 3+4	no	5.3	4.4	3.9	4.6	4.7	3
004	61	38.7	Gleason 4+3	yes	5.1	5.2	5.9	5.4	7.3	6.9
005	67	6	Gleason 3+4	yes	6.3	5.3	8.2	8.4	8.6	12.2
			Gleason 3+4	yes	3.8	4.5	5.6	5.9	4.9	6.5

* - For patient 1, due to technical failure, the pelvic portion of the PET4 could not be reconstructed.

Supplemental Table 2. Cohort B - mCRPC Patient Characteristics

	Patient Cohort (N = 15)
Median Age (range)	68 (35 – 85)
Prior Local Treatment (%)	
Radical Prostatectomy	5 (33)
Radiation	10 (67)
Median Time Since Start of Androgen Deprivation Therapy to Scan, months (range)	46.2 (10.5 – 102.4)
Prior systemic therapy (%)	
Abiraterone	8 (53)
Enzalutamide	4 (27)
Docetaxel	4 (27)
Sipeuleucel-T	3 (20)
Median serum PSA, ng/mL (range)	49.2 (0.7 – 1238.6)

Supplemental Table 3. Normal organ uptake for CTT1057 in mCRPC patients (n=15).

Organs	Median SUV$_{mean}$ (range)
Lacrimal	2.60 (1.66 – 7)
Parotid	3.94 (1.99 – 11.1)
Submandibular Gland	3.93 (2.36 – 7.34)
Blood pool	2.06 (0.89-3.47)
Liver	3.25 (2.14-4.07)
Kidney	8.66(3.62-13.5)
Spleen	2.86 (1.28 -3.63)
Duodenum	2.22 (1.05 – 5.1)
Bone marrow (Iliac crest)	0.75 (0.4-1.77)
Pancreas	1.54 (0.73-2.27)